First-principles investigation of the assumptions underlying model-Hamiltonian approaches to ferromagnetism of 3*d* impurities in III-V semiconductors

Priya Mahadevan and Alex Zunger
National Renewable Energy Laboratory, Golden, Colorado 80401, USA
(Received 15 August 2003; published 24 March 2004)

conductor. As the holes are not confined to the impurity band

crystal with the impurity atom. For example, while in GaAs:Co the hole has a dominantly t_2 character, the corresponding isoelectronic impurity ZnSe:Fe has a hole with e symmetry.

(

GaN. We used a Monkhorst Pack grid of $4\times4\times4$ k points which includes . The cell-internal positions of the atoms were allowed to relax to minimize the forces. The equilibrium transition metal-to-As bond lengths in GaAs were 2.47, 2.47, 2.48, 2.44, 2.36, and 2.34 Å for V, Cr, Mn, Fe, Co, and Ni, respectively.

The *d* partial density of states as well as the local moment at the transition-metal were calculated within a sphere of radius of 1.2 Å about the atoms, and have been broadened with a Gaussian of 0.2 eV full width at half maximum. The total energy differences were computed for TM pairs at first and fourth neighbor separations for parallel ferromagnetic) and antiparallel antiferromagnetic) arrangements of their spins to determine whether a specific transition metal impurity resulted in a ferromagnetic state or not.

LDA vs GGA: In order to compare LDA Ref. 30) and GGA Ref. 28) exchange functionals, we consider the case of Co impurity in GaAs, where earlier LDA work[12] suggests a nonmagnetic ground state. Using the experimental lattice constant of 5.65 Å for GaAs, we find that the GGA calculations lead to a magnetic ground state with a moment of 2 $_B$. The energy of this state is strongly stabilized by $\sim$150 meV compared to the nonmagnetic state. Using a LDA exchange functional we find that while the nonmagnetic state is stabilized for a $2\times2\times2$ Monkhorst-Pack grid as used in the earlier work,[12] the magnetic state with the moment of 2 $_B$ is stabilized by $\sim$40 meV for a $4\times4\times4$ Monkhorst-Pack k point grid. These observations are consistent with the fact that GGA calculations have a greater ability to stabilize a magnetic ground state than LDA calculations. For other impurities, such as Cr and Mn in GaAs, the LDA and GGA results are found to give the same ground state. We use the GGA exchange functional throughout this work.

The introduction of various transition-metal impurities lead to defect levels in the band gap of the semiconducting host. We compute the formation energies of the transition-metal impurities in various charge states *q*. The formation energy for a defect comprising of atoms in the charge state *q* was computed using the expression[31]

$$\Delta H_f,^q \equiv \Sigma \quad \Sigma \quad \Sigma$$

atoms on which each of the t_2 states are localized by computing the atom-projected DOS. Bonding states with a large wave function amplitude on the TM site are referred to as crystal field resonances (CFRs),[1] whereas antibonding t_2

splittings of the CFR and DBH levels at the Γ point for the impurities V-Co in GaAs obtained from an analysis of their eigenvalues and eigenfunctions. For V and Cr the spin splitting of the DBH levels is positive, i.e., t_+^{DBH} states are at lower energies compared to t_-^{DBH}. However, for Mn, Fe, and

occupiedasinV

significantly less TM character being dangling bond hybrids). This is discussed next.

1) *Anticrossing of the two t_2 levels in different host materials:* Level anticrossing is evident when keeping the impurity atom fixed, and, changing the host semiconductor. Considering the example of Mn, we find that by changing the host from GaSb to GaN, the DBH and CFR exhibit anticrossing. This is not the only difference: We find that the exchange splitting of the DBH levels is in the same direction as the CFR levels positive) in GaN:Mn, in contrast to GaAs:Mn. Further, in GaN:Mn the t_+^{CFR} levels lie above the e_+^{CFR} levels, unlike the case in GaAs:Mn. The reason is evident from Fig. 4, which shows that the VBM of GaN is much deeper than the VBM of GaAs. Since the free Mn^{2+} ion has its *d* orbitals *above* the GaN VBM, but *below* the VBM of GaSb or GaAs, an anticrossing occurs along the GaN $\rightarrow$GaP$\rightarrow$GaAs$\rightarrow$GaSb series. This is illustrated in Fig. 5, which shows that in GaN:Mn for the up-spin channel, the upper t_2 is more localized than the lower t_2, whereas in GaAs:Mn the localization sequence is reversed. This clarifies a confusion that existed in the literature[42] regarding the question of whether the gap 9.978 0gap 9.978 0gap 9Ar6o]TJ9(oeh3232(Ga8.
td54221.2(clafyto54221.7(the)4221.nerature)4221.5(of54221.7(the)4221.a

states in II-VI's, the experimental result should be compared with the total energy difference between the configurations d^4 and d^5 and not with the bare single particle eigenvalues. Alternatively, the LDA error can be empirically corrected by using the simplified LDA+U version of the SIC. In Fig. 6 we plot the Mn t_+^{CFR} partial density of states as a function of U for GaAs:Mn. As U increases, the position of the Mn related levels and therefore the t^{CFR} level is pushed deeper into the GaAs valence band. Agreement with x-ray photoemission spectroscopy (XPS) for the t_+^{CFR} being at $E_v - 4$ eV occurs for U $\sim$ 2 eV. As U increases, the CFR levels t_2 and e are pushed to deeper energies (larger binding energy), become spatially more localized and increase their exchange splitting. On the other hand, the DBH level becomes more delocalized, has less Mn character, lower exchange splitting. This is because the energy separating the Mn d levels and the dangling bond levels increases with U, as a result of which the effective coupling between Mn and the host-like states decreases. The T_c is consequently reduced. The picture of a ''hostlike hole'' obtained for unphysically large U leads to nearly vanishing FM stabilization energy. Clearly, the picture of ''hostlike hole'' is invalid for GaAs:Mn, since for the U that leads to agreement with XPS the DBH hole is still localized to some extent, whereas for very large U, when the hole is delocalized, there is no ferromagnetism.

C. The perturbed host VBM

Having studied the impurity-induced levels in the gap and deep in the host valence band, we next examine the perturbation of the host states, especially the host valence band maximum by the presence of the impurity atom. Figure 7 shows the up- and down-spin band dispersions for a 3% Cr doped GaP supercell [panels (a) and (b)]. The band dispersion of the GaP host without the impurity has been provided in panel (c) for comparison. The thickness of the lines depicting these bands has been made proportional to the Cr d character of the states. We see that Cr introduces a new band within the band gap of GaP. In a band-theoretic picture, this system is metallic, with the Fermi energy within the impurity band.

Interestingly, (1) the host band dispersions are significantly altered by the presence of the impurity. In particular the VBM is found to have a significant TM d character for the 3% Cr concentration represented by the supercell, (2) A Cr-induced spin splitting of the valence band maximum is observed. Effects (1) and (2) suggest that the host VBM is sufficiently perturbed by the transition metal.

Another way of detecting perturbations in the host bands is to examine the host projected DOS of the system containing the impurity. In Fig. 8 we plot the As p partial density of states projected onto different As atoms labeled 1–4 for a GaAs supercell containing two Mn atoms. The As atom labeled 1 has one Mn nearest neighbor, while the As atom labeled 2 has two Mn nearest neighbors. The As atoms show a strong polarization which increases with the number of Mn neighbors. The As atoms labeled 3 and 4, which are far away from the Mn atoms, show a 0 TD90il-332.9(polarizatioO.2(detectarizatIc
ciims

adjoining chains the perturbation is limited in extent. Further

sumed in model Hamiltonian theories (reviewed in Sec. I) is consistent with first-principles calculations (outlined in Sec. IV).

(i) *The nature of the TM-induced hole state*: A $3d$ impurity in a III-V semiconductor generates two sets of states with t_2 symmetry, and one set of states with e symmetry in each spin channel. While one set of t_2 states are localized on the TM atom (CFR), the other are localized on the host anion atoms next to the impurity (DBH). These states CFR and DBH exhibit an anticrossing for a fixed TM as a function of the host anion GaN→GaP→GaAs→GaSb, or for a fixed host as a function of the impurity V→Mn. The localization of the hole state decreases as we move from Mn in GaN to Mn in GaP, and then to Mn in GaSb. Not all impurities introduce holes. In GaAs, V^0 and Fe^0 have no hole; Cr^0, Mn^0, and V^- have t_2 holes; and Fe^- has an e hole. In all cases, however, the hole is nonhydrogenic, manifesting a significant admixture of $3d$ character and showing deep acceptor levels whose energies do not follow the host VBM. This implies that the neglect of the short-range part of the impurity potential and the consequent expansion of the acceptor wave function in terms of a single host wave function are questionable. The effective mass of the hole state is therefore different from that of the host, as observed in recent experiments.[46] The exchange splitting of the CFR states is different for the t_2 states from that for the e states. While the splitting for the e states is larger than that for the t_2 states for V and Cr in GaAs, the order is reversed for Mn, Fe, and Co. This reversal in the order of the spin splitting of the CFR states is accompanied by a reversal in the sign of the spin splitting of the DBH states. The identity of the hole state—both the symmetry as well as the character—depends on the impurity-host combination. While the hole carrying orbital for Fe in ZnSe has e symmetry, the hole is found to be located in an orbital with t_2 symmetry for the isovalent doping of Co in GaAs.

(ii) *The nature of the host VBM*: The introduction of the

ization between the anion dangling bonds generated by a column III cation vacancy V_{III} [i) above], and the crystal-field and exchange-split d levels of a TM ion placed at the vacant site [ii) above]. There are two limiting cases: When the $3d$ levels are well below the host cation dangling bonds e.g., Mn in GaAs, Fig. 11), or when the $3d$ levels are well above the host cation dangling bonds e.g., V in GaAs, Fig. 12). The dangling bond states are shown on the right hand side of Figs. 11 and 12, while the crystal field and exchange

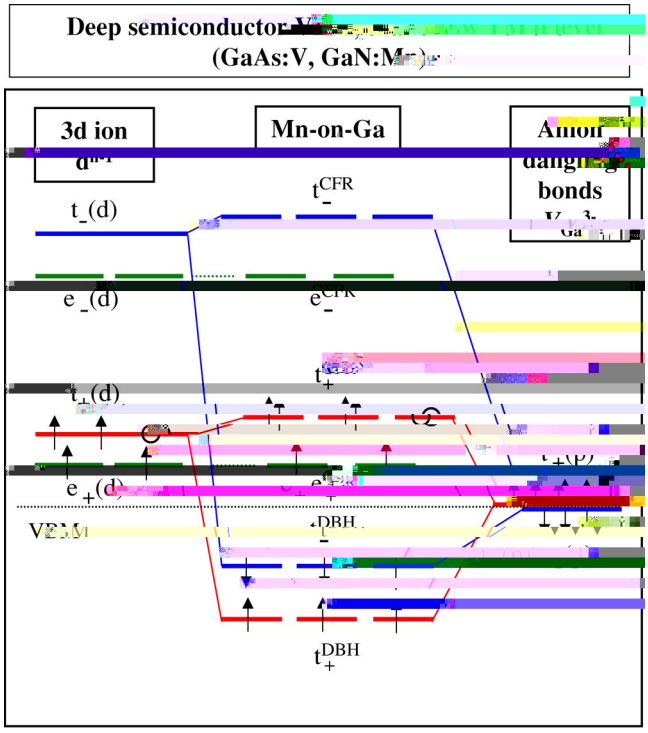

FIG. 12. Color online) The schematic energy level diagram for the levels central panel) generated from the interaction between the crystal-field and exchange-split split levels on the 3*d* transition metal ion left panel) with the anion dangling bond levels right panel), when the TM *d* levels are energetically shallower than the dangling bond levels.

Fig. 11). The number of electrons $(n-1)+6$ is 10, 11, and 12 for Mn, Fe and Co, respectively. This agrees with Fig. 1 showing that Mn and Fe in GaAs have the ordering of levels shown in Fig. 11, with fully filled t_+^{CFR} and e_+^{CFR} levels and 2, 1, and 0 holes in the t_+^{DBH} level. By an analysis of the density of states obtained within our first-principle calculations, we have determined Table III) the energy minimizing orbital configurations for the transition, metal impurities V, Cr, Mn, Fe, and Co in GaAs in fully relaxed configurations. The first unoccupied orbital for each impurity has been indicated in boldface in Table III. The simple model of Figs. 11 and 12 gives the same result.

B. Qualitative consequences of the simple model

1) *Level anticrossing*: The model explains how the hopping interaction between the t_2 states on the transition-metal impurity with the cation-vacancy states generates a pair of t_2 states in each spin channel. The bonding-antibonding character of these states is determined by the relative separation of the interacting levels as well as their interaction strengths. Hence, as depicted in Fig. 14, one could by a suitable choice of the TM impurity change the character of the gap levels. When the orbital energy of the 3*d* ion lies below the host dangling bond, we have a ''CFR-below-DBH'' situation, illustrated in Fig. 11. In this case one has CFR states in the valence band of the semiconductor while the gap

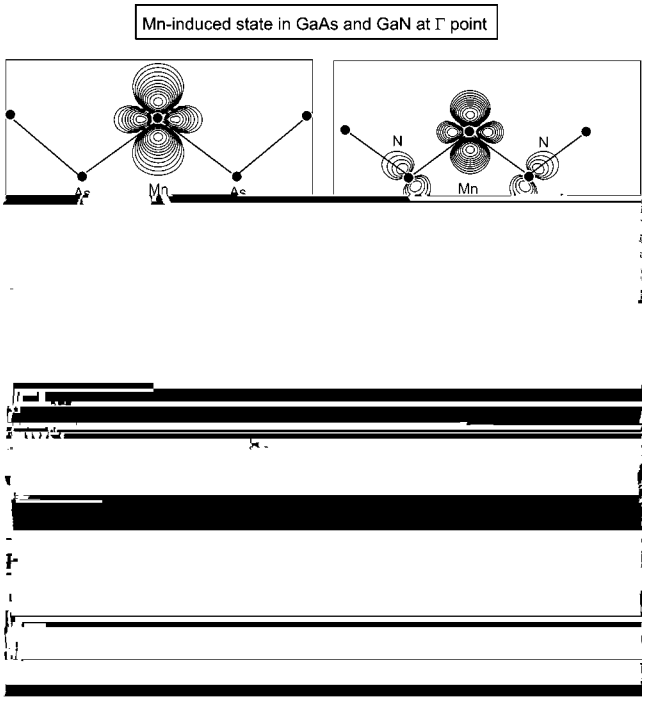

FIG. 13. The wave function squared of Mn induced a) e^{CFR} in GaAs:Mn, b) e^{CFR} in zinc blende GaN:Mn, c) t^{CFR} in GaAs:Mn, d) t^{CFR} in zinc blende GaN:Mn, e) t^{DBH} in GaAs:Mn, and f) t^{DBH} in zinc blende GaN:Mn. The lowest contour corresponds to $0.015e/Å^3$ and each contour is 1.6 times larger.

levels are more delocalized with dominant weight in the dangling bonds. This is the case for GaAs:Fe, Mn, and Co. Conversely, when the orbital energy of the 3*d* ion lies *above* the host dangling bond, we have the ''CFR-above-DBH'' situation, illustrated in Fig. 12. In this case the gap level is CFR-like.

While Fig. 1 illustrates anticrossing when changing the 3*d* atom, but keeping the host fixed, e.g., GaAs, Fig. 5 suggests that there is also anticrossing when keeping the 3*d*

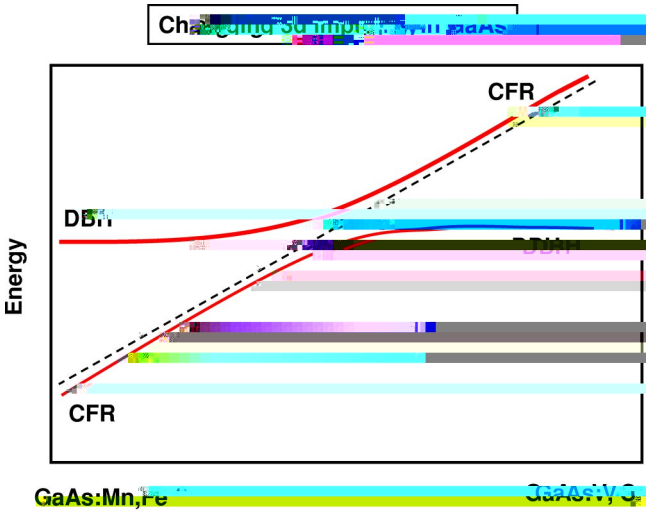

FIG. 14. Color online) The schematic plot of band anticrossing between the two t_2-like levels in GaAs for different 3*d* impurities.

atom fixed, e.g., Mn, but changing the host crystal GaN →GaP

automatically from such a microscopic model. The perturbation of the host valence band is not directly related to the coupling strength J_{pd}. When the hole has primarily a DBH character, one finds the perturbation of the host valence band is larger. The basic picture that emerges from our first-principles calculations could be used to replace the more naive model Hamiltonian treatments which have assumed a hostlike hole picture, an unperturbed valence band, and a spin of the hole that couples to the spin of the TM via a local exchange interaction.

ACKNOWLEDGMENT

This work was supported by the U.S. DOE, Office of Science, BES-DMS under Contract No. DE-AC36-99-G010337.

---

[1] See A. Zunger, in *Solid State Physics*, edited by F. Seitz, H.

Opin. Solid State Mater. Sci. **5**, 261 (2001).
[37] B. Beschoten, P.A. Crowell, I. Malajovich, D.D. Awschalom, F. Matsukura, A. Shen, and H. Ohno, Phys. Rev. Lett. **83**, 3073 (1999).
[38] T. Komori, T. Ishikawa, T. Kuroda, J. Yoshino, F. Minami, and S. Koshihara, Phys. Rev. B **67**, 115203 (2002).
[39] E. Tarhan, I. Miotkowski, S. Rodriguez, and A.K. Ramdas, Phys. Rev. B **67**, 195202 (2003).
[40] S.H. Wei and A. Zunger, Appl. Phys. Lett. **72**, 2011 (1998).
[41] M.J. Caldas, A. Fazzio, and A. Zunger, Appl. Phys. Lett. **45**, 671 (1984).
[42] T. Dietl, Semicond. Sci. Technol. **17**, 377 (2002).
[43] J. Okabayashi, A. Kimura, O. Rader, T. Mizokawa, A. Fujimori, T. Hayashi, and M. Tanaka, Phys. Rev. B **58**, 4211 (1999).
[44] A. Zunger, Phys. Rev. Lett. **50**, 1215 (1983).
[45] S.B. Zhang, S.H. Wei, and A. Zunger, Phys. Rev. B **52**, 13975 (1995).
[46] E.J. Singley, R. Kawakami, D.D. Awschalom, and D.N. Basov, Phys. Rev. Lett. **89**, 097203 (2002).
[47] G.B. Bachelet, G.A. Baraff, and M. Schluter, Phys. Rev. B **24**, 915 (1981).
[48]